

論文 / 著書情報  
Article / Book Information

Title	A study on neutron emission from a cylindrical inertial electrostatic confinement device
Author(s)	N. Buzarbaruah, S.R. Mohanty, E. Hotta
Citation	Nuclear Instruments and Methods in Physics Research Section A: Accelerators, Spectrometers, Detectors and Associated Equipment, Vol. 911, pp. 66-73
Pub. date	2018, 11
DOI	<a href="http://dx.doi.org/10.1016/j.nima.2018.09.076">http://dx.doi.org/10.1016/j.nima.2018.09.076</a>
Creative Commons	See next page.
Note	This file is author (final) version.

# License



Creative Commons: CC BY-NC-ND

# **A Study on Neutron Emission from a Cylindrical Inertial Electrostatic Confinement Device**

**N. Buzarbaruah<sup>1</sup>, S.R. Mohanty<sup>1\*</sup>, E.Hotta<sup>2</sup>**

<sup>1</sup>Centre of Plasma Physics-Institute for Plasma Research, Nazirakhat, Sonapur, Assam, India

<sup>2</sup>Tokyo Institute of Technology, 4259-J2-35 Nagatsuta, Midori-ku, Yokohama 226-8502, Japan

## **Abstract:**

The adaption of new generation portable neutron sources has been increasingly marked in a wide range of research fields compared to the large-scale neutron generators. In this context, we have successfully demonstrated some of the essential parameters required for the emission of 2.45 MeV DD fusion neutrons from a steady state portable linear neutron source based on inertial electrostatic confinement scheme. The parameters that control the production of neutrons are the working pressure of the fuel gas, applied voltage, measured current and cathode geometries. The neutrons emitted from the source are confirmed using neutron monitor, bubble dosimeters, nuclear track detectors and He-3 proportional counter. Presently, we can produce neutrons up to the order of  $\sim 10^6$  n/sec at discharge voltage ranging from -60kV to -80kV and discharge current of 20mA to 30mA.

## **I. Introduction:**

In the present world, artificial neutron sources play a crucial role in paving the way for various potential applications. The portable or tabletop neutron sources are relatively inexpensive alternatives to the nuclear reactors [1, 2]. The neutrons produced from such sources are used in different fields of science such as electronics industries, medicinal fields, homeland security and other research areas [3-5]. Lawrence Berkeley National Laboratory (LBNL) and Adelphi Technology Inc. are the pioneers for the development of a series of high yield neutron generators using D-D (deuterium fuel) reactions in an axially symmetric device [6].

Inertial electrostatic confinement (IEC) fusion scheme is one of the most favorable techniques for production of continuous and pulsed neutrons compared to other schemes like plasma focus, Z-pinch, accelerator-based etc. Researchers have analyzed various schemes for IEC devices that could deliver a stable source and could significantly increase the neutron

production rate (NPR) and the density of oscillating ions in the core region of the cathode [7, 8]. An IEC device is configured both for spherical (isotropic) and cylindrical (anisotropic) geometries, running by an electrical discharge on D–D/D–T/D–<sup>3</sup>He as fuel gases. It primarily consists of a gridded electrode acting as cathode at the center of a vacuum chamber serving as the anode. A glow discharge plasma takes place between the electrodes due to the high voltage breakdown of the fuel gas, thereby, producing ions that are accelerated towards the cathode. The ions produced travel in radial trajectories and circulate through an open spherical or cylindrically gridded cathode, the electrons remain between the gridded cathode and the anode. The radial distribution of ion density, mainly interior to the cathode, and formation of a deep potential well is of key significance for the occurrence of fusion regimes in the cathode grid [9]. Theoretical studies using simple analytic models have indicated that such systems cannot scale to net energy producing devices [10]. The highly efficient electrostatic systems and combinations of both magnetic and electrostatic arrangements are applied for the production of neutrons. Scientists from various prominent institutes of the world that include University of Wisconsin (UW) Madison, Los-Alamos National Laboratory (LLNL), University of Illinois, Kyoto University and Tokyo Institute of Technology (TITECH) in Japan are pioneers of initializing the IEC concept and allocated the concept of gridded IEC devices, from the earlier ion and electron gun concepts of Hirsch and Farnsworth [7, 11]. The researchers of these organisations are continuously performing experiments related to the production of neutrons, protons, high energy photons (Gamma rays) and other fundamental aspects of the sustainable development of IEC devices. For increasing the amount of neutron flux and NPR following the IEC fusion scheme, the suitable modification was made in the designing and operating methodologies that resulted in the development of devices such as spherically convergent beam focus (SCBF), radially convergent beam focus (RCBF), spherically convergent ion focus (SCIF). The SCIF device at Wisconsin University achieved a higher range of fusion reaction rates up to  $10^8$  n/s for D–D fuel and  $10^{10}$  n/s using D–T fuel [12, 13]. The SCBF device at TITECH developed a scheme for accelerating ions which are generated between electrodes by a glow discharge, towards the spherical center and giving rise to fusion reactions. The device has recorded up to  $10^6$  n/s in steady-state operation and  $10^9$  n/s in a pulse mode of operation [14]. G.H. Miley and his colleagues at the University of Illinois first used the single gridded IEC device and recorded a neutron output up to  $\sim 10^6$  to  $10^7$  neutrons/sec when operated with a steady-state deuterium discharge of 70 kV, 15 mA [15]. From the experimental observations of University of Wisconsin (UW) and Illinois, the net fusion energy output from IEC like systems is  $10^{-5}$  times lesser than the input energy [16].

Radel et al. reported on steady-state neutron outputs from the spherical IEC device of UW. The authors experimentally verified that there are three main parameters available to change the neutron output in an IEC device of a specific anode/cathode size configuration: cathode voltage, power supply meter current, and fusion fuel density (gas pressure) [17]. The researchers at UW have increased the power rating of operation from 15 kW to 60 kW to take advantage of increased D-D fusion cross sections at higher voltages [18]. The ability to enhance the power rating could explore the usefulness of IEC devices as a source of neutrons in commercial applications.

In this paper, we discuss the parameters that are involved in the occurrences of fusion reactivity in the cylindrical IEC device that regulates the production rate of neutrons. In the first section, we tried to interpret the equations involved in defining the ion-neutral (beam-background) reaction regime that enhances the ion density profile and NPR from the device [19]. It has been reported earlier about the different reaction mechanisms of neutron productions such as beam-beam, beam-background, beam-cathode and fast-neutral-background collisions [13, 20]. The reactions mentioned above specify the interaction between the fast ions beams generated in the potential well due to the application of the high negative voltage to the transparent cathode grid. In the same section, we also discussed the dependence of NPR on the applied potential ( $\phi$ ) to the cathode grid, the discharge current ( $I$ ) and the neutral background pressure ( $n_g$ ). In the second section, we described the experimental setup and the different types of diagnostics used for measuring the count rate of neutrons produced due to DD fusion reactions. The mono-energetic deuterium ions generated from the cathode discharges are accelerated towards the cathode due to the inertia of the negative electrostatic field in between the cathode grid and chamber wall that subsequently, starts oscillating inside the negative potential well [21]. Thus fusion reactions take place between the counter-flowing ions forming a dense core inside the cylindrical cathode grid and between the ions and the background gas (beam-background) outside the gridded cathode [16]. The paper also discusses the increment of neutrons from the device and for which it is expected that low-pressure operation is effective where high voltage can be applied safely to the cathode reducing the formation of arc discharges and safe operation of the device. Due [to the higher convergence](#) of ions at the core, its density increases along with the collision frequency, and as a result, the NPR scales up gradually [22]. The dose rate of the neutrons, NPR and energy of the emitted neutrons were verified and examined using various neutron diagnostics that are discussed in section IV.

## II. Theoretical analysis:

The reaction regimes inside the electrically driven (current discharge) IEC device is mainly dependent on beam-background reaction of fuel ions. Thus the volumetric NPR arising from a mono-energetic population of energetic ions and background gas is given by [23, 24]

$$\frac{dN}{dt}(NPR) = n_c n_g (\sigma v) \text{-----} (1)$$

$n_i$  = ion density inside the device,  $n_g$  = background gas density,  $\sigma$  = fusion cross-section,  $v(r)$  is the relative velocity of the ion beams oscillating radially in the transparent gridded cathode region. The term  $(\sigma v)$  also resembles the fusion reaction rate, i.e., the distribution of ions and those taking part in the fusion reactions. The recirculation of ions impact upon the loss mechanism that occurs due to ion hitting the grid wires (mostly in beam-background and beam-cathode reactions). Due to the said phenomena, the ion scattering cross-section is higher than the fusion scattering cross section and the probability of higher fusion rate decreases. The total energy equivalence persists on  $E = -q\phi(r)$ , where  $q$  is the charge of the electron and  $\phi(r)$  is the high input potential applied to the cathode grid.

The ion flow characteristics inside the potential well depends on the applied current ( $I_T$ ) and potential to the cathode. The oscillating ions traversing throughout the cathode grid initiates a current given by the flow convergence model of ions [25]. The relation between the total applied current and the counterflowing ions is given by the recirculating factor of ions:

$$\xi = \frac{I_R}{I_T} \text{-----} (2)$$

$I_R$  is the recirculation current carried by the ions between the chamber wall and cathode space, and  $I_T$  is the total applied current at the cathode.

So, due to the recirculation of the ions in the grid, some secondary electrons would get emitted from the grid due to the impact of the ion into it. Therefore, the measured current in the cathode is given by

$$I_{meas} = I_T + I_T \delta_e = I_T (1 + \delta_e) \text{-----} (3)$$

Further, considering that the ions make some trips inside the cathode and so the recirculation current can be estimated as a measure of all the cathode currents that enhances the beam-

background reaction inside the cylindrical IEC device. If  $\eta$  is considered as the geometrical transparency factor and  $I_T$  remains as the cathode ion current,  $\eta I_T$  is the ion current to the core,  $\eta^2 I_T$  will be the ions that re-enter the inter-electrode space. So after adding all the ion terms that take part in the recirculation and encrypt the beam-background reaction is

$$\begin{aligned}
 I_R &= I_T + \eta^2 I_T + \eta^4 I_T + \dots \\
 I_R &= I_T \sum_{n=0}^{\infty} \eta^{2n} \\
 \therefore I_R &= \frac{I_T}{1-\eta^2} \text{-----(4)}
 \end{aligned}$$

Therefore, from equation (2)

$$\xi = \frac{I_R}{I_T} = \frac{1}{1-\eta^2} \text{-----(5)}$$

Again, the total core current is given by  $I_c = \eta I_R$  -----(6)

Relating equations (3), (4), (5) and (6) we have,

$$I_c = \frac{\eta I_{meas}}{(1-\eta^2)(1+\delta_e)} \text{-----(7)}$$

To increase the density of the fuel ions ( $D^+$ ) for increased fusion reaction rate, a collisionless model of ions (primary ion flow conversion model) has been formulated by Thorson et al. [13]. The model explicitly demands that the current carried by the ions at the core ( $I_c$ ), permitting the reaction mechanism to be proportional to the core ion density ( $n_c$ ). The current conservation model gives us

$$I_c = 2\pi r_c h q n_c v_c(r) \text{-----(8)}$$

Thus, ion density at the core  $n_c$  is given by

$$n_c = \frac{I_c}{2\pi r_c h q v_c(r)} \text{-----(9)}$$

Here,  $I_c$  is the ion current at the core,  $r_c$  and  $h$  are the radius and height of the core region of the cathode (the core radius is considered to be 1/10 of the cathode radius) [22, 23],  $q$  is the charge of the electron, and  $v_c$  is the core ion velocity. The typical diameters used in the present case of study are 0.02 and 0.03 m. The cathode used had a fixed length of 0.35 m and

transparency factor is 84.7% (8 wire grids) and 92.3% (16 wire grids). The input voltage 100 kV with ion core velocity ( $v_c$ ) of  $3.162 \times 10^6$  m/s and 1mTorr –  $3.30 \times 10^{19}$  m<sup>-3</sup>.

Table 1: Dependence of current at constant potential on the Neutron Production Rate (NPR)

Pressure (mTorr)	Ion currents (A)				Core radius ( $r_c$ ) m	Cathode transparency ( $\eta$ )	Fusion cross section ( $\sigma$ ) m <sup>2</sup>	Ion density ( $n_c$ ) m <sup>-3</sup>	NPR n/s
	$I_r$	$I_f$	$I_{meas}$	$I_c$					
0.7		0.169		0.142	0.001	84.7%		$1.49 \times 10^{15}$	$1.89 \times 10^{10}$
1	0.050	0.230	0.1	0.204	0.0015	88.5%	$4 \times 10^{-31}$	$2.15 \times 10^{15}$	$2.72 \times 10^{10}$
1.5		0.337		0.299	0.002	92.3%		$3.15 \times 10^{15}$	$3.98 \times 10^{10}$

The above table illustrates the dependences of ion currents that are calculated using the standard equations. The current assimilation, i.e., the core current is mainly dependent on the measured current ( $I_{meas}$ ) and transparency of the cathode. Thus, the relation facilitates the increase of ion current at the core ( $I_c$ ) and thereby increases the density of ions in the core. This increment scales up the fusion reactivity of ions and production of neutrons in the core.

### III. Experimental Set-up and Diagnostics:

The IEC device used in the present study consists of a cylindrical cathode grid kept inside a cylindrical stainless steel chamber of 50 cm in diameter and 30 cm in height placed vertically. The chamber has multiple ports for evacuation, viewing windows, high voltage feedthrough, gas inlets and coupling different diagnostics. The schematic of the experimental device is shown in Fig. 1, the top port of the chamber is used as an access port for high voltage feedthrough, and one side port is dedicated for coupling to the evacuation system. The cathode grid is made up of stainless steel with varying dimension and transparency. The design of cathode grid is made by simulation (SIMION 8.0) results and grid wire after analyzing the recirculation of ions the wired frequency had been optimized at 8 and 16. The diameters of cylindrical cathode grid used in the present study are 2 and 3 cm, and the length of the cathode is 25 cm, respectively [19]. The chamber was evacuated using a turbo molecular pump (TMP) backed with a rotary pump and the pressure inside the chamber has been monitored using the cold and capacitance gauges. The neutral deuterium gas was supplied using a deuterium gas generator, and the flow rate was controlled using a gas dosing valve supplied with a coarse feed valve.

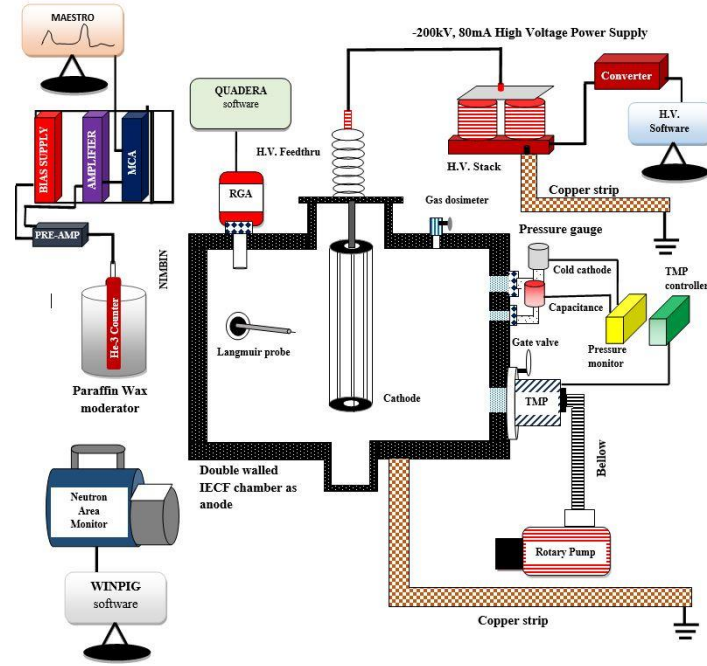


Fig. 1: Schematic of the cylindrical IEC device along with the associated accessories.

As mentioned above, in the present experiment we implemented the cold cathode plasma discharge to create deuterium plasma. The  $D^+$  ions are produced through electron impact ionization of the ambient gas (deuterium) inside the IEC chamber due to high voltage breakdown, and are trapped with negative electrostatic fields inside the cylindrically gridded cathode. While being accelerated in such a high electrostatic field, the ions not only gain fusion grade energy but also converge at the core region of the central cathode grid forming dense ion plasma at the core of the cathode region. The ions are oscillating in the negative potential well formed in the transparent cylindrical cathode. The primary fusion reaction for the present cylindrical IEC device is given by equation (10).



The signatures of neutron emission were noticed during the operation of the device in the voltage range of -20 kV to -100 kV using a high voltage power supply (HVPS). The diagnostics that are mainly implemented for confirming the evidence of neutrons from the steady-state linear neutron source are neutron area monitor, solid state nuclear track detector, i.e., CR 39 (Columbia Resin-39), bubble detector and He-3 proportional counter. The area monitor, made by KWD Nuclear Instruments (2222A model), has an inbuilt He-3 proportional counter embedded with polyethylene and boron plastic as moderator for detecting the thermal neutrons. The instrument is coupled with a microprocessor, memory functions, and real-time clock to serve as a general-purpose instrument for continuous

monitoring of neutron radiations in locations where permanent dose monitoring is required. The monitor measures the neutron dose rate in the unit of mSv/h in the energy range of 0.025 eV to 17 MeV and independent of the direction of the source. The monitor converts the energy of the thermal neutrons through an electronic driver and displays the direct reading of neutron dose rate (in the range of 0.001 mSv/h to 999 mSv/h) in the digital display of it or can be measured through interfacing software WinPig. The software provides a broader interface for analyzing dose rate, dose, and the dose rate log of neutrons. To characterize the DD neutron emission from the IEC device, we also used the nuclear track detector (NTD). These NTD contain hydrogen (H), carbon (C) and oxygen (O), and so the most relevant technique to detect fast neutrons is based on elastic scattering of neutrons on light nuclei, resulting in a recoil nucleus. Since neutrons do not directly cause any ionization in the detector, no tracks are produced by them. The neutron scatters elastically and give rise to recoil protons or production of charged particles that cause ionization, and consequently, etchable tracks. These NTD can record the impression of charged particles by the radiation-induced damage caused along the path of interaction. The damaged regions are developed for visualization with an optical microscope using a technique known as chemical etching [26]. Here, PM-355 (Pershore Mouldings), a super grade form of CR-39 NTD, was used and samples of size  $10 \times 20$  mm with a density of  $1.30 \text{ g/cm}^3$  were then placed at different distances from the neutron source (IEC device). After exposing the CR-39 samples to DD neutrons for about 5 minutes, they were etched by 6.25 N NaOH solutions at  $70 \pm 2 \text{ }^\circ\text{C}$  for an etching time of 6 hrs [27]. The etching solution was mechanically stirred to achieve a constant etching condition such as temperature and concentration of the solution. After etching, the detectors were viewed under an Olympus-made optical microscope equipped with a digital scanning firewire CCD camera. The track images of the detectors were acquired by CCD camera, and the images were analyzed using image analysis software. Another, non electronic detector viz. bubble detector was used for measuring the dose of neutrons of the IEC source. The bubble detector or bubble dosimeter is procured from BTI Bubble Technologies. These dosimeters are the most sensitive and provide accuracy for instant visible detection and measurement of neutron doses [28]. The detector contains tiny droplets of superheated liquid called Freon dispersed throughout a transparent polymer. As soon as the energetic neutron strikes the droplet, it instantly vaporizes, forming a visible gas bubble trapped in the gel. The bubble provides the measurement of the tissue-equivalent neutron dose. The detector has the sensitivity of 1 bubble/ $\mu\text{Sv}$  for neutrons and has sensitivity to gamma radiations, although having a limited validity of 90 days from the date of

calibration. To calculate the neutron counts and energy of the neutrons, we employed the He<sup>3</sup> proportional counter. These counters are useful to both count the particles and to discriminate between them based on the size of the pulse height each produced. The main advantages of He-3 detectors for neutron detection are the very high efficiency (resulting from its high thermal neutron absorption cross-section) and good discrimination of the gamma signal [29]. The detector procured from LND, USA is an SS tube of diameter 2.54 cm and active length 15 cm. It is placed inside a wax moderator of diameter 10 cm for interacting thermalized neutrons. Other electronics associated with the detector for obtaining the information regarding energy and counts of the radiated or charged particles through pulse height analysis (PHA) are pre-amplifier, amplifier and multi-channel analyzer (MCA).

#### **IV. Results and discussion:**

As mentioned earlier the experimental evidence of DD fusion neutron emission from the cylindrical IEC device is ascertained by using multiple diagnostics and the results obtained from them are discussed hereafter.

##### ***(i) Detection of neutron by area monitor***

Experiments were performed to study the neutron emission from the cylindrical IEC device. Cold cathode deuterium plasma discharge was initiated at low voltage (-2 kV), high chamber pressure (15 mTorr) and kept the discharge for 30 min to remove the impurities in the wires of the cathode grid. After optimizing the gridded cathode at lower voltages, we applied high voltage from -60 kV to -80 kV by keeping the chamber pressure at 0.7 mTorr to 1 mTorr. Figure 2 (b) and (c) illustrates the formation of DD fusion-grade plasma in the inner core of the cylindrical grid at a fixed voltage of -60 kV and the measured current of 10 mA and 30 mA, respectively. From the visual appearances of Fig. 2 (c), it is observed that as increasing the supply current to the cathode more number of ions are interacting with the surface of the grid wires of the cathodes and secondary electrons are produced from the surface of the grid wires. The interaction of the highly energetic D<sup>+</sup> ions (60 keV) heats up the surface of the grid wires, illuminating more light from the core area of the grid. Thus the current generated at the core is the sum of the ion current ( $I_i$ ) and the electron current ( $I_e$ ). Both  $I_i$  and  $I_e$  play a crucial role in driving the recirculation of ions inside and near the grid, formation of the space charge potential and multiple potential wells [16, 30].

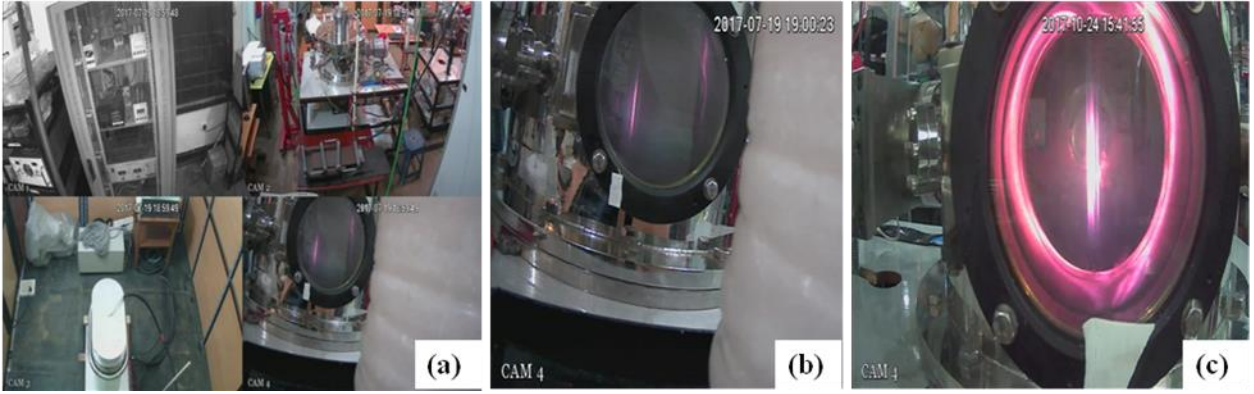


Fig. 2: (a) Images of the IEC neutron source along with other subsystems. (b) Glow from a linear stream of fusion plasma formed inside the cylindrical grid-cathode at -60 kV, 10 mA operations. (c) Intense glow from the core of the cathode at -60 kV, 30 mA.

The electronic assembly converts the counts or yield of neutrons into dose equivalent (Sieverts or rem). The monitor is kept at a radial position from the source at a distance of 60 cm from the cathode. The dose rate is displayed in the software window of the detector for -60 kV, 10 mA (Fig. 3(a)) and -60 kV, 30 mA (Fig. 3(b)) discharges. In our experiment, as shown in the dose rate window of Fig. 3(a) and (b), the NPR increases with respect to the input power.

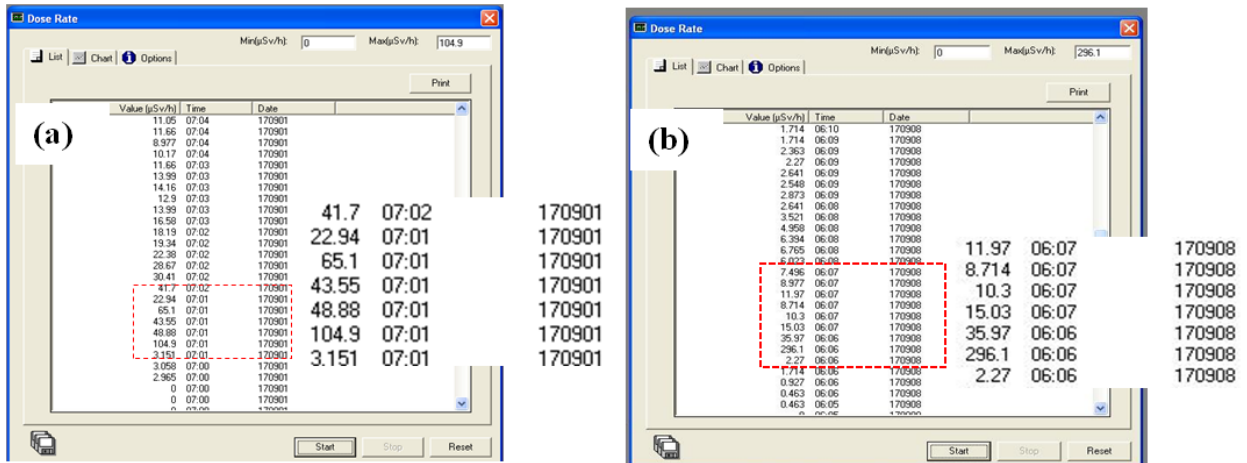


Fig. 3: Dose rate window of the WinPig software (a) at -60kV, 10mA discharge. (b) At -60kV, 30mA.

On analyzing the dose rates of neutrons from the area monitor, it can be noted that on increasing the total ion current from the supply unit the core current and the recirculation rate of the ions increases to scale up the fusion process and thereby neutron dose rate increases. The neutron monitor was also calibrated to a known source Am-Be which delivered NPR of  $\sim 10^6$  n/s calculated by noting the dose rate, distance from the source and conversion factor ( $2.15 \mu\text{Sv hr}^{-1} \text{cm}^2 \text{s}$ ) and the distance from the source. From this conversion factor, the total

NPR has been obtained in the present case where the source strength is unknown. So, we used some theoretical equation which served the basis of calculating the NPR.

The relation between NPR and dose rate can be expressed as [31]:

$$D_0 = h_E \phi \text{-----(11)}$$

Here,  $D_0$  is the equivalent dose for the source,  $h_E$  is the fluence to dose conversion factor, and  $\phi$  is the neutron flux. In order to calculate neutron flux at a typical experimental condition (60 kV, 30 mA and 0.7 mTorr) we used the dose rate shown in Fig. 3(b).

$$D_0 = 296.1 \mu\text{Sv hr}^{-1}, h_E = 2.15 \mu\text{Sv hr}^{-1} \text{ cm}^2 \text{ s}$$

Thus from equation (11), and putting the above values we obtain flux ( $\phi$ ) as  $137.72 \text{ cm}^{-2} \text{ s}^{-1}$  at a distance of 60 cm from the source. The neutron flux is used to extrapolate NPR using following equation.

$$\text{NPR} = 2\pi r^2 \phi \text{-----(12)}$$

After putting the respective values in equation (12), we obtained the NPR to be  $3.1 \times 10^6 \text{ n/s}$ . We have examined the dependence of NPR with the filling gas pressure of deuterium and the discharge current. The plot shown in Fig. 4 indicates the increase in the production rate of neutrons from the source with the increase of current as well as filling gas pressure. It is noteworthy to mention that the device is continuously operated for 10 min at 60 kV applied voltage without damaging grid assembly.

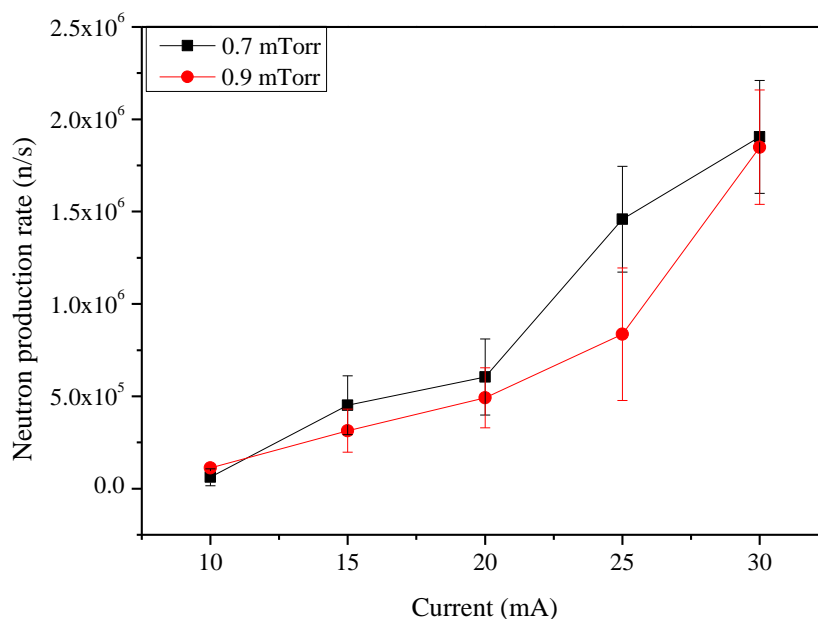


Fig. 4: Variation of neutron production rate with filling gas pressure and the discharge current

***(ii) Detection of fusion neutrons by proton recoil methods:***

Apart from the above mentioned electronic detectors the flux of fast neutrons can also be determined using specific non-electrical detectors namely NTD (CR-39). On occurrence of the HV plasma discharge DD neutrons scatter elastically, and produce recoil protons or carbon or oxygen nuclei in CR-39 while interacting with it. However, all detected tracks are indeed due to protons as the scattered carbon and oxygen ions have a short range in CR-39 due to their higher masses. Figure 5 (a) shows the reference sample, i.e. the unexposed but etched (6 hours) CR 39 plate and Fig. 5 (b) shows the plate exposed to neutrons ( $\sim 10^6$  n/s) and etched in NaOH solution up to 6 hours. The tracks formed in the plate are visible and shows some dark, round and oval tracks. The oval-shaped track is expected due to oblique incidence of neutrons. On increasing the current levels 10 mA and 30 mA, working pressures 0.9mTorr and 0.7mTorr while keeping the voltage fixed at -60 kV the number of tracks increased (Fig. 5(c) and 5(d)) and revealed the increase in neutron flux from the cylindrical source. We exposed CR39 to DD neutrons for 10 min at discharge voltage and current -60 kV and 30 mA, respectively. After performing chemical etching for 6 hours, tracks are noticed in exposed CR39 detectors shown in Fig. 5 (c). While comparing the present result with the earlier result, we observed that the number of tracks increases (from 57 tracks to 156 tracks) on increasing the power to the grid.

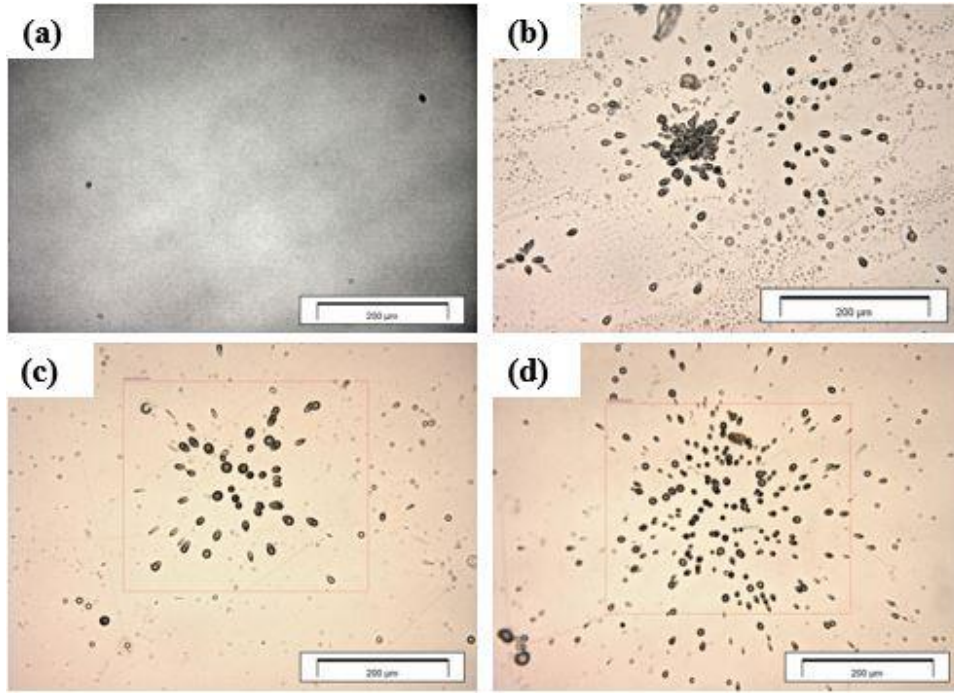


Fig. 5: Formation of neutron induced tracks on CR39 (a) Unexposed and etched CR 39 sample, (b) Exposed sample of CR 39 and formation of neutron irradiated tracks, (c) Exposure to low flux of neutrons at 0.9 mTorr, -60 kV and 10 mA, (d) Exposure to high flux of neutrons at 0.7 mTorr, -60kV and 30 mA.

***(iii) Detection of fusion neutrons by bubble dosimeter:***

To further verify the observation of neutrons from the cylindrical IEC source, we employed non-electronic bubble detector (BD-PND). The bubble detector was fixed to one of the windows of IEC device as shown in Fig. 6 (a). The filling gas pressure of 0.7 mTorr was maintained inside IEC chamber and H.V. of up to  $-60$  kV, 10 mA was applied to the cathode grid. We found the development of bubbles in the detector as a result of incident neutrons in contact with the liquid droplets of the detector. The photograph shown in Fig. 6 (b) clearly shows the appearance of the detector before and after neutron exposure. As per the calibration reports of the detector using a known Am-Be source 1 bubble is equivalent to  $1 \mu\text{Sv}$  of radiation dose. In our case when we exposed the dosimeter at  $-60$  kV, 10 mA, the number of bubbles appeared was 11, and as soon as we increased the measured current to 30 mA, the number increased to 13, i.e. recording the dose rate to  $13 \mu\text{Sv}$ . Thus, we have successfully reported in recording the neutron dose from the cylindrical IECF source using bubble detectors.

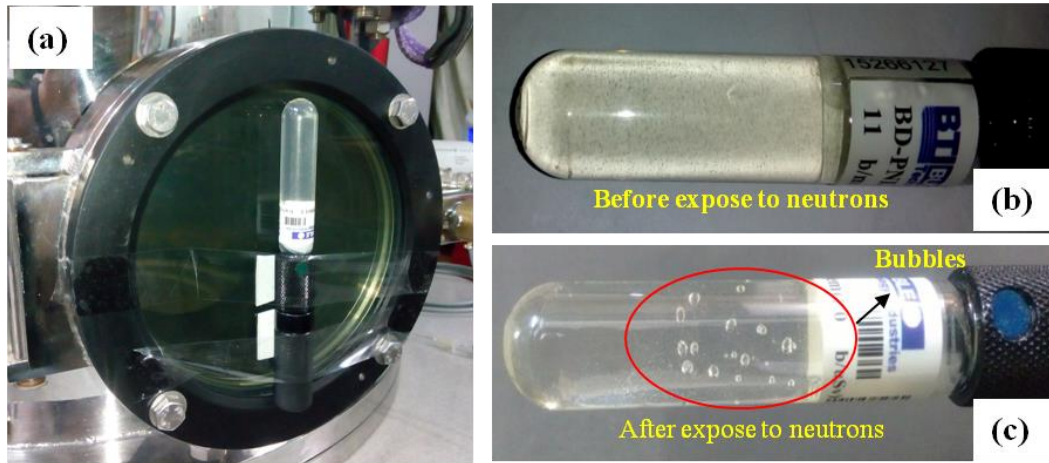


Fig. 6: (a) A typical photograph of the bubble detector placed in the front window of the IEC chamber (b) The exposed and unexposed bubble detectors to neutrons from the IEC chamber

**(iv)  $He^3$  proportional counters:**

The detectors mentioned in the earlier sub-sections are used for recording both the thermal neutrons (0.025 eV) in area monitor and fast neutrons (2.45 MeV). So, to study the DD neutron counts and energy of the emitted neutrons from the linear source we employed the He-3 proportional counter. The fast neutrons lose their initial kinetic energy and get attenuated in paraffin wax moderator and the  $^3He$  captures the thermalized neutrons. The slow neutron induced reactions which serves the basis for the conversion of neutrons to directly detectable charged particles is given by equation (13) mentioned below:



The pulse height spectra of incident thermal neutrons were analyzed in multi-channel analyzer (MCA) which requires the supporting electronics viz. power supply, preamplifier, and amplifier. Figure 7 (a) shows the nuclear instrumentation module (NIM Bin) with associated supporting electronics for the detector. The pulse height spectrum (PHS) of the background was initially recorded and shown in Fig. 7 (b). After observing the background pulses discharge was initiated and PHS of DD neutrons was recorded. It is observed that the pulse height appeared at channel number 1050 (shown in Fig. 7 (b)) corresponds to the total energy output of the above reaction (equation (13)) i.e. 764 keV. This pulse height is indicative of that the device emits 2.45 MeV fusion neutrons.

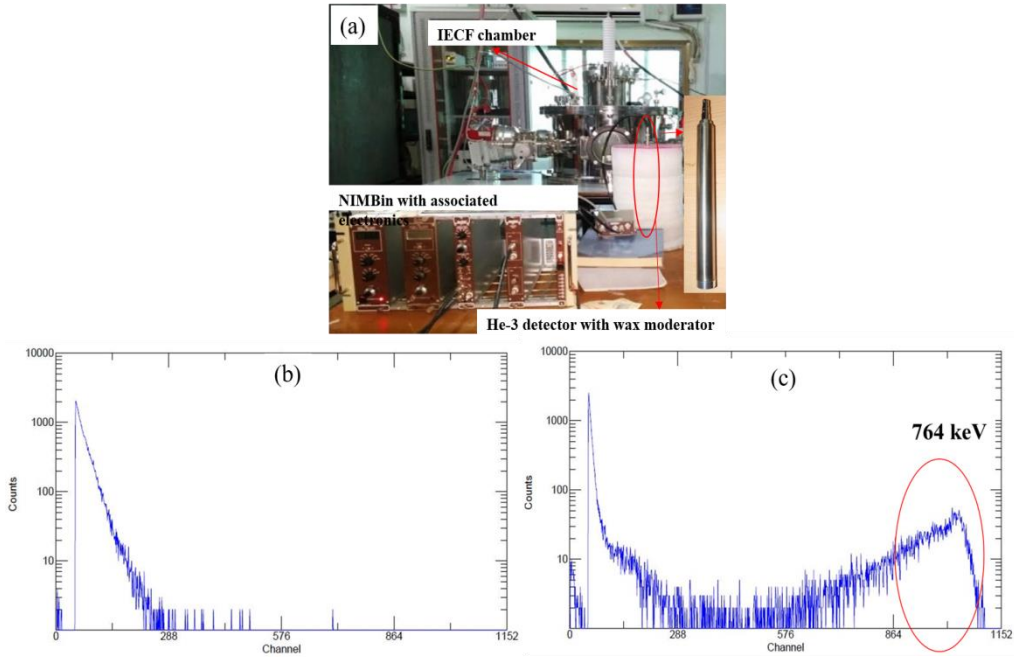


Fig. 7: (a) Neutron detection using  $^3\text{He}$  proportional counter and associated electronics, (b) Background spectra of the He-3 counter (c) Pulse height spectra of neutrons formed in the He-3 proportional counter.

## V. Conclusion and summary:

The emission of DD neutrons from a table top cylindrical IECF device has been successfully monitored using various detectors. The NPR of  $10^6$  n/s at an applied voltage of -60 kV has been estimated in the present work. It has been proven that the NPR depends not only upon the discharge current but also on the filling gas pressure. The neutron emission from this source can be scaled up by introducing higher applied voltage up to 100 kV and reducing the filling gas pressure below 0.7 mTorr. Nevertheless other challenges like suppression of micro-arcs in the cathode region, external corona discharge along the high voltage cable routing, grid heating due to the increase in grid potential and interaction of energetic ions to the surface of the grid etc. need to be overcome for such high voltage operation. Future work will concentrate on operation of the device above 100 kV addressing the said challenges.

## Acknowledgments:

The authors are grateful to the Director, Institute for Plasma Research (IPR), Gandhinagar, India and Centre Director, Centre of Plasma Physics-Institute for Plasma Research (CPP-IPR),

Sonapur, India for support to carry out the present work. The technical assistance of M.K.D. Sarma has been appreciated.

## References:

- [1] G.H. Miley, A portable neutron / tunable X-ray source based on inertial electrostatic confinement, *Nucl. Instr. Meth. Phys. Res. A* 422 (1999) 16–20.
- [2] G.L. Kulcinski, Overview of neutron/proton source applications from IEC fusion devices, *Trans Am Nucl Soc* 77 (1997) 507.
- [3] G.H. Miley, L. Wu, H.J. Kim, Nuclear techniques in national security studies on contraband detections IEC-based neutron generator for security inspection system. *J Radioanal Nucl Chem* 263 (2005) 159–164.
- [4] K. Yoshikawa, K. Masuda, T. Takamatsu, Y. Yamamoto, H. Toku, T. Fujimoto, E. Hotta, K. Yamauchi, M. Ohnishi, H. Osawa, S. Shiroya, T. Misawa, Y. Takahashi, Y. Kubo, T. Doi, Research and development of the humanitarian landmine detection system by a compact fusion neutron source, *IEEE Trans. Nucl. Sci.* 56 (2009) 1193–1202.
- [5] Y. Takahashi, T. Misawa, C. Pyeon, S. Shiroya, K. Yoshikawa, Landmine detection method combined with back scattering neutrons and capture g-rays from hydrogen, *Applied Radiation and Isotopes* 69 (2011) 1027–1032.
- [6] N. Marchese, A. Cannuli, M.T. Caccamo, C. Pace, New generation non-stationary portable neutron generators for biophysical applications of Neutron Activation Analysis, *Biochimica et Biophysica Acta* 1861 (2017) 3661–3670.
- [7] R.L. Hirsch, Inertial-electrostatic confinement of ionized fusion gases, *J. Appl. Phys.* 38 (1967) 4522–4534.
- [8] A.L. Wehmeyer, R.F. Radel, G.L. Kulcinski, Optimizing neutron production rates from D–D fusion in an inertial electrostatic confinement device, *Fusion Sci Technol* 47 (2005) 1260.
- [9] K. Yoshikawa, K. Takiyama, T. Koyama, K. Taruya, K. Masuda, Y. Yamamoto, T. Toku, T. Kii, H. Hashimoto, N. Inoue, M. Ohnishi, H. Horiike, Measurement of strongly localized potential well profiles in an inertial-electrostatic fusion neutron source, *Nucl Fusion* 41 (6) (2001) 717–720.
- [10] D.C. Barnes, R. A. Nebel, Stable, thermal equilibrium, large-amplitude, spherical plasma oscillations in electrostatic confinement devices. *Phys Plasmas* 5 (1998) 2498.
- [11] P.T. Farnsworth, Electric discharge device for producing interaction between Nuclei, US Patent No. 3,258,402 (1966).

- [12] G.H. Miley, Y. Gu, J. DeMora, M. Ohnishi, Accelerator plasma-target-based fusion neutron source, *Fusion Engineering and Design* 41 (1998) 461–467.
- [13] T.A. Thorson, R.D. Durst, R.J. Fonck, A.C. Sontag, Fusion reactivity characterization of a spherically convergent ion focus, *Nuclear Fusion*, 38 (1998) 4.
- [14] K. Tomiyasu, K. Yokoyama, K. Yamauchi, M. Watanabe, A. Okino, E. Hotta, Effects of cusp magnetic field in a cylindrical radially convergent beam fusion device, *Fusion Science and Tech.* 56 (2009) 967-971.
- [15] G.H. Miley and John Sved, The IEC-A Plasma-target-based Neutron Source, *Appl. Radiat. Iso*, 48 (1997) 1557-1561.
- [16] G.H. Miley, S. K. Murali, *Inertial Electrostatic Confinement Fusion Fundamentals and Applications*, 2014. doi:10.1007/978-1-4614-9338-9.
- [17] R.F. Radel, Detection of highly enriched uranium and tungsten surface damage studies using a pulsed inertial electrostatic confinement fusion device. Ph.D. thesis, Department of Engineering Physics, University of Wisconsin, Madison (2007).
- [18] B.B. Cipiti, The fusion of advanced fuels to produce medical isotopes using inertial electrostatic confinement. Ph.D. thesis, University of Wisconsin–Madison (2004).
- [19] N. Buzarbaruah, N.J. Dutta, J.K. Bhardwaz, S.R. Mohanty, Design of a linear neutron source, *Fusion Eng. Des.* 90 (2015) 97–104.
- [20] G.H. Miley, Y. Gu, J.M. DeMora, R.A. Stubbers, T.A. Hochberg, J.H. Nadler, G.H. Miley, R.A. Anderl, Discharge characteristics of the spherical Inertial Electrostatic Confinement (IEC) device, *IEEE Trans. Plasma Sci.* 25 (1997) 733–739.
- [21] N.Buzarbaruah, N.J.Dutta, D.Borgohain, S.R.Mohanty, H.Bailung, Study on discharge plasma in a cylindrical inertial electrostatic confinement fusion device, *Physics Letters A* 381 (2017) 2391–2396.
- [22] G.H. Miley, J. Nadler, T. Hochberg, Y. Gu, O. Barnouin, J. Lovberg, Inertial – Electrostatic Confinement: An approach to burning advanced fuels, *Fusion Technology*, 19(1991) 840-845.
- [23] M. Ohnishi, Y. Yamamoto, M. Hasegawa, K. Yoshikawa, G.H. Miley, Study on an inertial electrostatic confinement fusion as a portable neutron source, *Fusion Engineering and Design* 42 (1998) 207–211.
- [24] Irving Kaplan, *Nuclear Physics*, Addison-Wesley Publishing Company, Menlo Park, California, Chap.18 (1977) 578.
- [25] T.A. Thorson, R.D. Durst, R.J. Fonck, L.P. Wainwright, Convergence, electrostatic potential, and density measurements in a spherically convergent ion focus, *Phys. Plasmas* 4 (1997) 4-15.

- [26] F. Castillo, G. Espinosa, J.I. Golzarri, D. Osorio, J. Rangel, P.G. Reyes, J.J.E. Herrer, Fast neutron dosimetry using CR-39 track detectors with polyethylene as radiator, *Radiation Measurements* 50 (2013) 71-73.
- [27] M. Bhuyan, N. K. Neog, S. R. Mohanty, C. V. S. Rao, and P. M. Raole, Temporal and spatial study of neon ion emission from a plasma focus device, *Physics of Plasmas* 18 (2011) 033101.
- [28] E. Ramalho, L. Reina, A. X. da Silva, A. Facure, Bubble Detector's Evaluation For Neutron Field Measurements In A Very Known Source, 2011 International Nuclear Atlantic Conference - INAC 2011, ISBN: 978-85-99141-04-5.
- [29] R. Batchelor, R. Aves, and T. H. R. Skyrme, Helium-3 Filled Proportional Counter for Neutron Spectroscopy, *Review of Scientific Instruments*, 26 (1955) 1037.
- [30] K. Noborio, Y. Yamamoto, Y. Ueno, S. Konishi, Confinement of ions in an inertial electrostatic confinement fusion (IECF) device and its influence on neutron production rate, *Fusion Engineering and Design* 81 (2006) 1701–1705.
- [31] G.F. Knoll, *Radiation Detection and Measurement*, 4th Ed, published by John Wiley and Sons (2010) pp 121-128 and 655-664.